CONFERENCE PRE-PRINT Topic: EX-C

PULSE DESIGN SIMULATOR FOR JT-60SA

E. JOFFRIN,
CEA, IRFM, F-13108 Saint-Paul-lez-Durance, France.
Corresponding author email: emmanuel.joffrin@cea.fr

J.F. ARTAUD, G. FALCHETTO, G. GIRUZZI
CEA, IRFM, F-13108 Saint-Paul-lez-Durance, France.

M. MATTEI, D. FRATTOLLILO,
Università di Napoli Federico II and CREATE Consorzio, via Claudio 21, 80125, Napoli Italia

L. DI GRAZIA
CREATE Consorzio, via Claudio 21, 80125, Napoli Italia

C. BOULBE, B. FAUGERAS
Université Côte d'Azur, CNRS, INRIA Castor, LJAD, Parc Valrose, 06108 Nice Cedex 2, France

W. BIN
Consiglio Nazionale delle Ricerche (ISTP-CNR), via R. Cozzi 53, 20125 Milano, Italia

M. IAFRATI
ENEA - C.R. Frascati - Via Enrico Fermi, 45 00044 Frascati (Roma)

A. MELE
École Polytechnique Fédérale de Lausanne Rt Cantonale, 1015 Ecublens (VD) Switzerland

M. SCHNEIDER
ITER-Organisation, Route de Vinon sur Verdon, 13115 St Paul Lez Durance, France

Abstract

A pulse design simulator (PDS) has been designed for JT-60SA. The PDS has the goal to offer a practical tool for the scientists and operators to prepare plasma scenario within the technical limits of the device. The tool is based on the fast kinetic code METIS [1] coupled with the free boundary code and controllers adapted for the different phases of the discharges. An innovative numerical method is applied for the coupling between METIS and the free boundary code NICE [2]. The magnetic controllers are relying on simple linearized models describing the dynamic behaviour of the plasma, the active control circuits, and the currents flowing in the surrounding conductive structures. The PDS has been tested successfully on the 4.6MA/2.25T discharge planned in the next operation phase of JT-60SA. It can be used by dedicated experts for designing the new scenarios of the future campaign of the machine.

1. INTRODUCTION

In the operation of modern tokamaks and future large machines, scientists and control room operators will develop their plasma scenario before proposing or implementing their experiment. They should rely on a reliable and realistic tool for the design of plasma discharges. Such Pulse Design Simulator (PDS) should be capable of simulating a discharge from plasma breakdown to the very end of the discharge going through the start of ramp-up plasma, X-point formation, current flat top right to the ramp-down and include heating and transient phases (such as transition to H-mode or high plasma β, …). The PDS should also include machine operational constraints and limits (current limits, forces, voltage limits, etc …) that a specific scenario should comply with. At the same time, the tool should be sufficiently light in computing time and accessible to any person without requiring lengthy training.

With these requirements, we have designed and implemented a PDS for JT-60SA based on the coupling of time dependent kinetic calculations from the METIS [1] code with the free boundary equilibrium code NICE [2]. For this purpose, NICE-METIS has introduced a specific novel numerical method to ensure the coupling between the Grad-Shafranov equation and current diffusion [3]. The simulator integrates controllers implemented in Matlab Simulink for the plasma shape, vertical stabilization and plasma current [4] for all phases of the discharge including transient, such as ramp-up, ramp-down, X-point formation, L to H and H to L transition, perturbation mitigation. The same architecture for the pulse design simulator is also being developed for the WEST tokamak [5] and ITER. The simulator does not aim at describing transport with sophisticated high-fidelity codes. It uses a light formulation for « reproducing » plasma kinetic parameters such as the evolution of density, temperature and energy content (in

METIS). Nor is it a high-fidelity model for plasma discharges (e.g. it does not contain disruption models or sophisticated edge or fast particle models …).

In this paper, the simulator structure and components are first described. Then controllers design is explained and documented. In its first version, the simulator has been first tested on the Ip=5.5MA, B_T=2.25T (scenario 2 of the JT-60SA research plan). More recently it was also successfully tested on the whole 4.6MA/2.28T (q_{95}~3) H-mode scenario which is planned to be run in the next JT-60SA campaigns in 2026 or 2027 [6]. The first results are shown in the last section. This simulator was developed in a pragmatic way with modellers, control engineers and plasma operation specialists and is now addressing other JT-60SA scenarios like the hybrid scenario (2.7 MA/1.70 T, q_{95} ~ 4).

2. PULSE DESIGN SIMULATOR STRUCTURE

The Pulse Design Simulator is built on the basis of a set of interconnected tools (figure 1) designed for the preparation of experiments for the tokamak JT-60SA.

- The first step consists in the design of a set of coherent end to end plasma shapes sequence. The plasma scenario is designed with the METIS code [1] with the set of plasma shape from CREATE-EGENE as input. Both codes are synchronized on a plasma current reference as CREATE-EGENE does not include any evolution but provides only a set of independent snap-shot equilibria. The full description of the scenario is set in METIS by designing the references for main plasma parameters (plasma current, line averaged density, effective charge, toroidal magnetic field, heating powers, …) and also the model parameters (plasma composition, confinement scaling law, …).
- Then, the feasibility of this scenario with respect to coil current and forces is tested using the free boundary equilibrium code FEEQS [3] used in inverse mode and includes a cost function optimized for JT-60SA. FEEQS receives from METIS the plasma current (Ip), the profiles P' and FF' and, as a constraint, the set of points defining the Last closed flux surface (LCFS). Thanks to the optimized cost function implemented in the code, we get a complete free boundary equilibrium solution with a new LCFS and the coils currents. The new computed set of LCFS can be used in METIS to improve the prediction of the scenario and the coil currents prediction are used later as feed forward reference for the controller.
- Finally, for the full-time evolving scenario simulation including the plasma description provided by METIS, a free boundary MHD equilibrium code is used (CREATE-NL [7] or NICE [8]) together with the controller built in Simulink© (see next section).

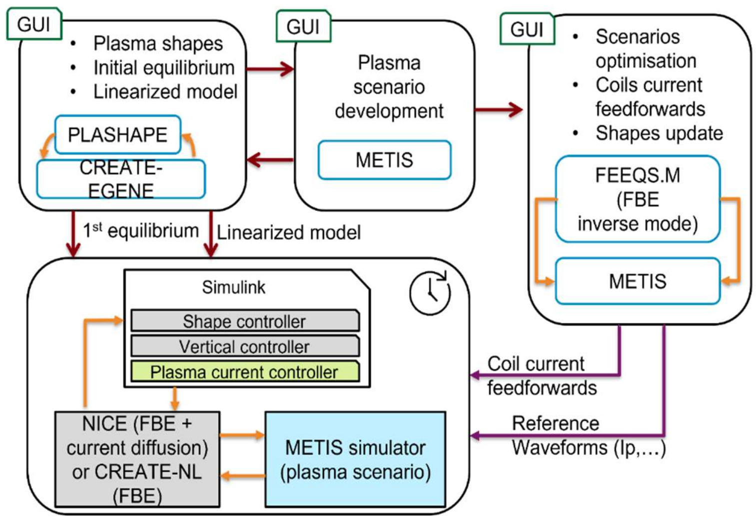

Figure 1: overview of the pulse design simulator structure

The full simulator is built on the coupling of three main components:

1) The plasma kinetic simulation from METIS
2) A free boundary equilibrium (FBE) code CREATE_NL or NICE. The FBE is used in "direct mode".
3) The Simulink© controllers (see next section). The controller for plasma shape, plasma current and vertical stability receives the observed plasma current, plasma geometry, gaps (either measured in poloidal flux differences or in real special distances), coils currents and it provides the voltages at the terminal connections of the coils. A kinetic controller for the control of plasma state which is also presently under development but not implemented yet for this contribution.

Before running the loop on time slices, the simulator requests an initial state. The initialization consists in a first call of METIS alone followed by a convergence loop between METIS and the FBE. Once a stable solution is obtained, a coherent state between the FBE and METIS is obtained. The feedforward references for the coil currents are updated to take into account the change and the controller can be initialized. The main simulator loop starts from this initialized state, then, it increments the internal time, calls the FBE code in direct mode and then METIS, computes the magnetic probe values and gaps between the plasma and the first wall and calls the controller that is either implemented as a Matlab function or a Simulink block diagram. The data are saved in files and memory after each time steps.

Initially, the FBE code CREATE-NL was coupled to METIS. METIS received the plasma last closed flux surface (LCFS), the value of the flux on the LCFS and the moments used internally by METIS equilibrium: the 1D profile of magnetic axis position and of flux surface elongation. Two numerical schemes have been used for coupling METIS with the FBE. In the first scheme, referred to as “light coupling”, the equilibrium profiles P’ and FF’ of the Grad-Shafravov equations are parametrized in a simple way by the plasma current Ip, the normalized pressure βp and the normalized internal inductance li [7]. This coupling the convergence as it acts as a space filter on the detailed features of P’ and FF’ profiles computed in the METIS code. As a consequence, this mode does not take into account details of the pressure profile such as the pedestal in case of H-mode or details of current density profile such as reversed q profile.

In the second coupling scheme, the so called “strong coupling”, the P’ and FF’ profiles provided by METIS code are directly used in CREATE-NL in addition to Ip. The convergence of this scheme is numerically more challenging than the previous light coupling and numerical instability and drift of boundary condition for the current diffusion equation were observed during the initial tests.

Indeed, the coupling of the Grad-Shafranov equation with the current diffusion equation [9] is challenging and has been dubbed “queer equations” [10]. Both equations are derived from MHD equations but the first does not have time evolution and the second is a 1D equation. Additionally, the poloidal flux is a coordinate in the first but the becomes the field to solve in the second. As a consequence, it is difficult to compute the FF’ profile and, more detrimentally, to define the boundary condition of the current diffusion equation. To solve this issue, an alternative numerical method where a pair of coupled equations for the MHD equilibrium and the evolution of the diamagnetic function F is solved [11] in NICE, thus providing a cleaner mathematical formulation. The NICE code was then coupled with METIS in the simulator workflow in the following way: first, NICE receives from METIS, the plasma current, the P’, the source of non-inductive current J_{ni} and the plasma parallel resistivity η and calculates the current diffusion. Then, METIS receives the whole equilibrium data from NICE including 1D and 2D data for the poloidal flux, magnetic field, metric coefficients, LCFS, and also scalar data such as Ip. The computation of the MHD equilibrium and current diffusion is disabled in METIS, but still continues to compute kinetic profiles (Pressure, n_e, T_e, T_i, …), sources (including J_{ni}) and the plasma resistivity. The first implementation of this new version of NICE showed some oscillations in the simulation results but have been overcome by using to the Hsieh-Clough-Tocher C1 finite elements [12].

In the process of testing the simulator, it was also observed that the current density profile was evolving towards very peaked profiles and high internal inductance. In an actual experiment, this type of profile condition triggers sawtooth that eventually flattens the current density profiles. In the case of the coupling between CREATE-NL and METIS a sawtooth model included in METIS. For coupling between NICE and METIS, the current diffusion is no more computed in METIS and a sawtooth mechanism had to be implemented to mimic sawtooth crash in this new workflow. This was done by modifying the source of non-inductive current J_{ni} and the plasma parallel resistivity the call of NICE. The resistivity is flattened inside the reconnexion zone. A perturbation to the non-inductive current J_{ni} is applied such that, after a time step, the safety factor become the one computed by the reconnexion model. In the present version of the simulator, the prescription of full reconnexion Kadomtsev model was used.

3. DESIGN OF THE CONTROLERS

The design of magnetic controllers is carried out of simple linearized models obtained with CREATE-EGENE [1] which implements both CREATE-L [13] and CREATE-NL+ [7] codes. These models describe the dynamic behaviour of the plasma, the active control circuits, and the currents flowing in the surrounding conductive structures in the neighbourhood of a given equilibrium point. Given a plasma equilibrium characterized by the value of the plasma current I_p and the current distribution, depending in first approximation on poloidal beta β_p and internal inductance li, the linearized model reads as follows:

$$L\delta\dot{x} + R\delta x = Su + L_E\delta w$$
$$\delta y = C\delta x$$

where δ denotes the variation of x or y with respect to the nominal equilibrium value x_0 or $y0$. $x = \left[I_{PF}^T \ I_{VSU} \ I_{VSL} \ I_e^T \ I_p\right]^T$ is the state vector of currents including active control currents $I_{PF} \in R^{n_{PF}}$ ($n_{PF} = 10$) in both the central solenoid CS and the external PF coils (see figure 2a), active currents I_{VSU} and I_{VSL} flowing in two in-vessel circuits which are dedicated to the plasma vertical stabilization, the vector of passive currents I_e induced in the surrounding structures (110 currents were adopted to take into account the main axial symmetric passive conductors). $u = [V_{PF}^T \ V_{VS}^T]^T$ is the vector of input voltages, $V_{PF} \in R^{n_{PF}}$ being the vector of voltages applied to the superconducting CS/PF circuits, and $V_{VS} = [V_{VSU} \ V_{VSL}]^T$ the vector of voltages applied to the in-vessel circuits. y is the output vector that holds all the quantities of interest for control, e.g., the plasma current and the currents in the active coils, as well as plasma shape and position descriptors; the poloidal magnetic flux and magnetic fields components in selected points. $\delta w = [\delta\beta_p \ \delta li]^T$ is the exogenous disturbance input to take into account the effect of plasma current redistribution during transients. L and R are the inductance and resistance matrix respectively, where the inductance matrix takes into account the presence of the plasma; L_E is the matrix linking the variation of exogenous inputs induced by the plasma current profile variations to the flux on the circuits. Finally, C is the output matrix and $S = [I \ 0]^T$ makes a selection of the circuits on which active voltages are applied.

The output vector includes plasma current, currents in the active coils (figure 2a), plasma to wall gaps [14], as well as the poloidal flux and fields on specified control points to control the plasma shape in the iso-flux control mode (see figures 2b, 2c, and 2d).

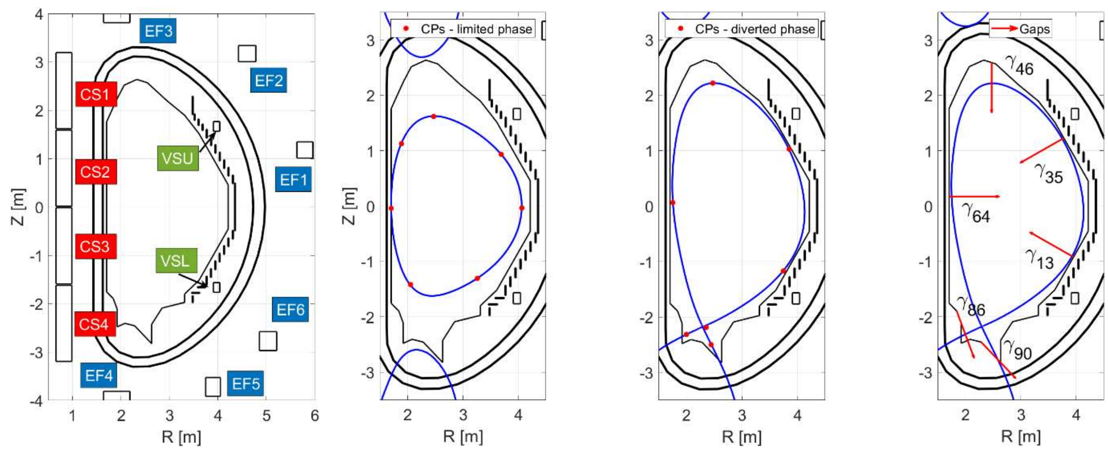

Figure 2a (left): JT-60SA poloidal cross-section with the poloidal coils – Figure 2b, 3c and 3d: Example of Control Points (CPs) on which to compute poloidal flux and fields for the limited plasma phase, and diverted plasma phase, and controlled gaps.

The overall magnetic controller [15] [16] [17] [1] reported in figure 3 is based on a Cauchy Condition Surface (CCS) scheme architecture, meaning that the plasma current and shape/position controllers request a PF/CS current variation to a lower-level PF current controller.

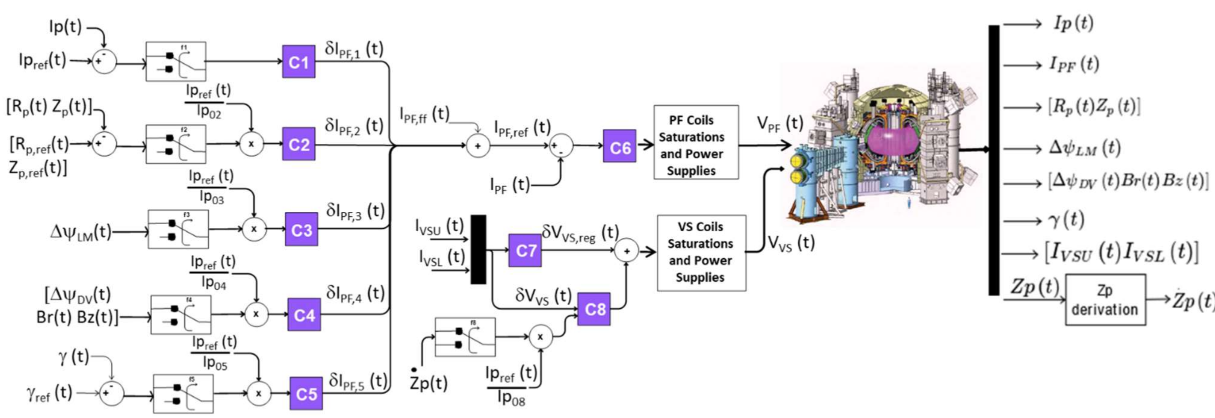

Figure 3 - Schematic view of the magnetic control architecture

Depending on the discharge phases, different combinations of controllers are needed. Logical commands are generated by a supervisor to activate the right combination based on time and plasma events (e.g. L-H transitions, X-point formation). Gains are scaled with the plasma current to compensate for the coil effectiveness variation.

The Plasma Current Controller (C1 in 3) tracks the plasma current reference $I_{p,ref}$ by generating a current request $\delta I_{PF,1}$ to the lower level current controller (C6) which adds to the nominal feedforward scenario control currents. Plasma current control is a SISO controller based on the so-called transformer pattern of current $I_{tr} \in R^{n_{PF}}$ which is optimized with the objective of controlling I_p minimizing the effect on plasma shape. A proportional-integral (PI) action has been considered with a settling time of about 3*s* this settling time is common to shape and position control.

The Plasma Centroid Controller (C2) tracks the plasma radial and vertical centroid position reference $[R_{p,ref} \ Z_{p,ref}]^T$ by generating the additional current request $\delta I_{PF,2}$. The radial and vertical position controller are two SISO controllers requesting two specific current patterns, namely I_r and $I_z \in R^{n_{PF}}$, that produce mainly a vertical/radial magnetic poloidal field using the external PF coils. Also, in this case a PI control action is adopted. For plasma shape control, an isoflux controller (C3) is used for the limited phase because the plasma wall distances (gaps) may be ill defined for low volume plasmas. This controller tracks the plasma boundary by controlling to zero the error between estimated flux on specified control points and the boundary flux ψ_b. It generates a request δI_{PF3} to the PFCC (PF Current Controller). Control gains are designed using a singular value decomposition approach and assuming that the request of currents is satisfied on a fast time scale. This approach is common to all the plasma shape controllers [18]. Plasma isoflux shape controller for the diverter phase (C4) brings to zero the difference between the estimated flux on the specified control points and the desired X-Point (XP) position boundary flux. In addition, the radial $B_{r,XP}$ and vertical $B_{z,XP}$ poloidal magnetic field components in the desired XP position are controlled to zero. This block generates request δI_{PF4} to the PFCC. Plasma gap controller (C5) tracks the reference plasma boundary by controlling to zero the error between the error on controlled reconstructed gaps $\gamma \in R^{n_\gamma}$, generating a request $\delta\, I_{PF5}$ for the PFCC. At the lower control level, the PF Current Controller (C6) guarantees that the currents in the superconducting PF circuits track the references $I_{PF,ref}$ which is the sum of the nominal feedforward currents and the requests generated by controllers (C1-C5). The PFCC Decoupling Controller exploits a well-assessed approach for the design of a Multi-Input-Multi-Output (MIMO) controller based on the superconducting active coils dynamic model [10]. The VS in-vessel coils are driven independently. To avoid an uncontrolled increase during the ramp-up of the mean value of the vertical stabilization VS circuits current $I_{VS,m} = 0.5 * (I_{VSU} + I_{VSL})$, a regularization control action (C7) is adopted to regulate it to zero with settling time equal to 1s. The Vertical Stabilization (VS) control action (C8) looks after the stabilization of the vertical elongated and unstable plasma column. The stabilization problem is reduced to a single-input-single-output problem (SISO), by using a linear combination of $I_c = 0.5 * (I_{VSU} - I_{VSL})$ and of the vertical speed of the plasma centroid $\dot{Z}_p$ as controlled variable. The VS is then designed as a proportional controller:

$$\delta V_{VS} = \begin{bmatrix} 1 \\ -1 \end{bmatrix} K_{VS} \ \left(k_I\, I_c + \dot{Z}_p\right)$$

where gains are obtained by solving a constrained optimization problem. The VS design explicitly accounts for the dynamic of the in-vessel coil power supply, which is modelled as a first order linear system in cascade with a pure delay: both the first-order time constant and the delay have been set conservatively equal to 2.5ms (which is almost the double of what have been estimated [19])

4. SIMULATOR RESULTS

To make a closed loop simulation of the 4.6MA diverted deuterium plasma JT-60SA scenario (see figure 4) an important preliminary step was to optimize nominal feedforward currents and nominal plasma shapes. A first guess of the nominal currents was provided by the FEEQS code [3] (see figure 5) as explained in section 2.

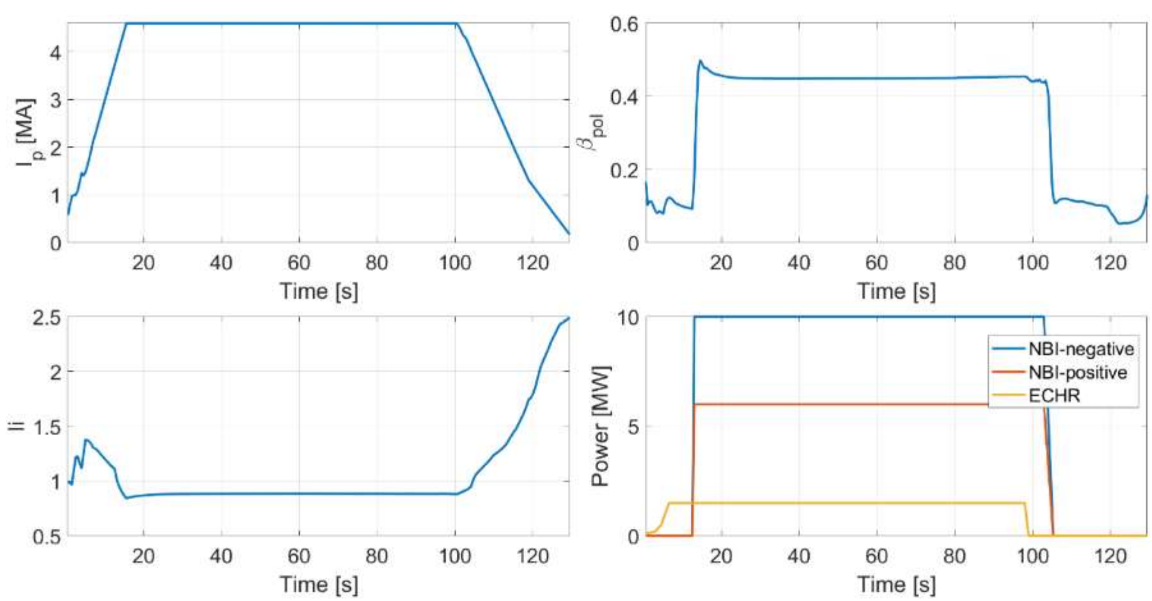

Figure 4 - Relevant global quantities for METIS simulation of the 4.6MA scenario: plasma current, poloidal beta, internal inductance and auxiliary power. The plasma composition is deuterium and carbon/oxygen as impurities.

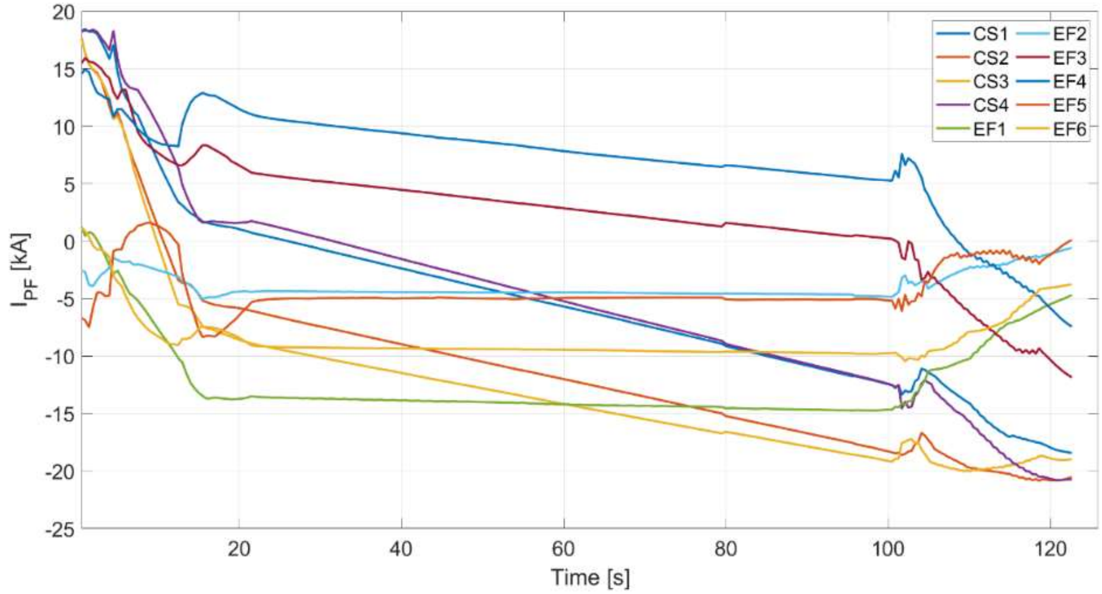

Figure 5 - FEEQS currents estimation for the 4.6MA scenario

Then free boundary equilibrium snapshots were produced using the CREATE-EGENE tool which was used to slightly modify plasma shapes and current to move the secondary upper X-point outside the chamber (see figure 6) and improve the plasma shape with respect to the inner wall and the upper X-point.

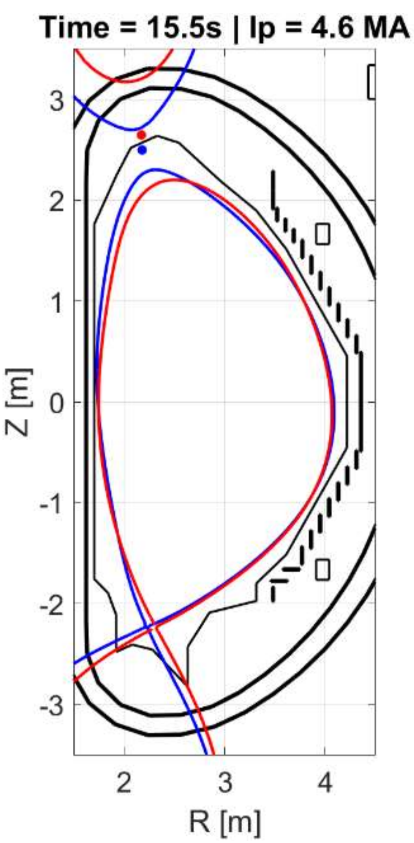

Figure 6 – Example of equilibrium modification for the 4.6MA scenario. The initial equilibrium (obtained using FEEQS current) is corrected to move the non-active upper X-point outside the chamber.

Linearized models were computed all along the scenario, to design and test the controllers with linear simulations. For the scenario, three controllers have been designed:

- During the early ramp-up phase (from 0.5s to 2.5s), the active controllers are the plasma current controller and the plasma centroid position controller.
- During the limited plasma ramp-up phase (from 2.5s to 4.5s), the plasma elongation is increased, therefore the VS controller is needed to cope with plasma vertical instability and the plasma centroid controller is switched off; the iso-flux shape controller is activated to keep increasing the elongation and to support the transition to the diverted phase.
- During the diverted plasma phase (from 4.5s to 126s) the plasma shape controller transitions from iso-flux for the diverted phase (from 4.5s to 10s) to gap shape control (from 10s to 126s).

A full NICE-METIS simulation has been run with the above controller in the loop. As one can see in figure 7, for the ramp-up the dynamic evolution differs from the expected one: METIS assumes shapes evolution coinciding to the reference one, however transients (e.g., eddy currents, plasma movements) and/or limits (e.g., active currents and voltages) are making the plasma evolution different from the nominal one. The magnetic controller can maintain satisfactory performance in the presence of model uncertainties, as shown by the plasma shape in figure 8, allowing to run a discharge from a low current limited plasma to high current diverted plasma during ramp-up and flat-top, keeping the currents and voltages within saturation limits. A few relevant shapes of this run are shown figure 9.

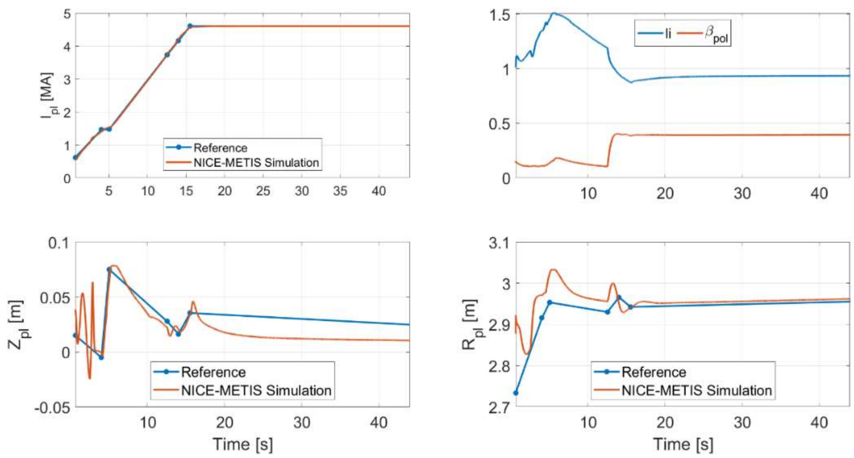

Figure 7 - Evolution of plasma current, internal inductance, beta poloidal, radial and vertical plasma centroid position during NICE-METIS simulation for the 4.6MA scenario.

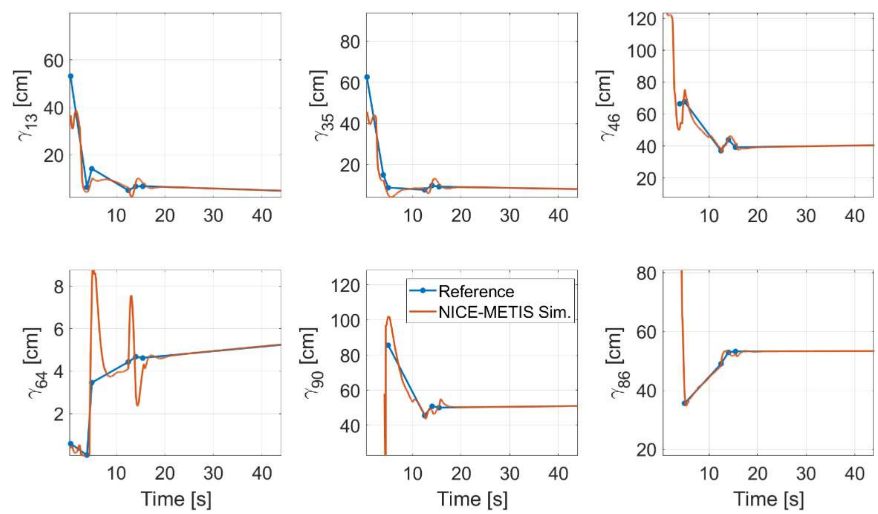

Figure 8 -Controlled gaps during NICE-METIS simulation for the 4.6MA scenario

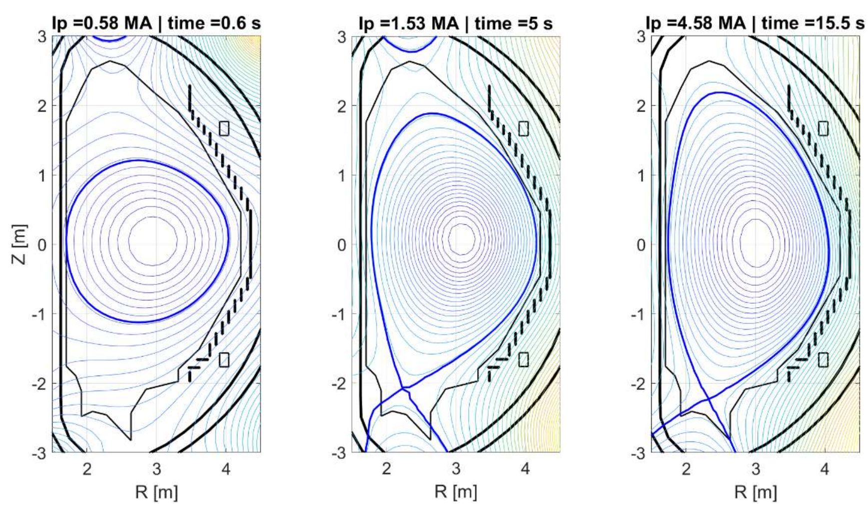

Figure 9 - Relevant plasma shapes during NICE-METIS simulation for the 4.6MA scenario.

With the PDS in this configuration, the pulse design simulation was eventually run for the whole duration of the high current (4.6MA) scenario in flux control using the controllers described above (figure 10).

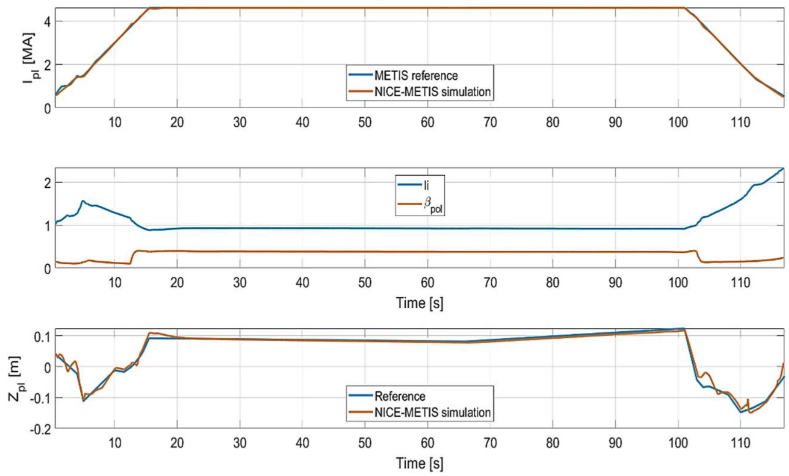

Figure 10: Simulation of the 4.6MA/2.25T scenario with the pulse design simulator with Ip (top), β, internal inductance (middle) and vertical position (bottom).

The pulse design simulator (PDS) and its controllers are now ready for use by dedicated expert users to proof-test the suite of codes and improve their robustness for the benefit to common users. The controllers used in the simulator have been designed in an ad hoc way, but the possibility exists to use those developed for the actual JT-60SA operation and tested in the first phase of operation of the machine (OP1) [20, 21] or future updates. It should be noted that at this stage tuning the controllers parameters still requires the assistance of a control engineer specialist. However, most of the tools have a user interface and therefore easy to use for other devices than JT-60SA such as WEST and ITER. The simulator runs on the EUROfusion Gateway and a user manual has been produced. The CPU time has not yet been fully optimized but this is the task of future work together with the expert users.

ACKNOWLEDGEMENTS

This work has been carried out within the framework of the EUROfusion Consortium, funded by the European Union via the Euratom Research and Training Programme (Grant Agreement No 101052200 — EUROfusion). Views and opinions expressed are however those of the author(s) only and do not necessarily reflect those of the European Union or the European Commission. Neither the European Union nor the European Commission can be held responsible for them.

REFERENCES

[1]: J.F. Artaud et al 2018 Nucl. Fusion 58 105001.
[2]: B Faugeras et al, Fusion engineering and design, Volume 160, November 2020, 112020
[3]: H. Heumann et al, J. Plasma Physics (2015), vol. 81, 905810301, doi:10.1017/S0022377814001251.
[4]: G. De Tommasi et al., 2024 Nucl. Fusion 64 076005
[5]: R. Nouailletas et al, Volume 192, July 2023, 113582 https://doi.org/10.1016/j.fusengdes.2023.113582
[6]: J. Garcia et al, this Fusion Energy Conference, Chengdu, IAEA 2025.
[7]: Albanese, R., Roberto Ambrosino, and Massimiliano Mattei. "CREATE-NL+: A robust control-oriented free boundary dynamic plasma equilibrium solver." Fusion Engineering and Design 96 (2015): 664-667.
[8]: B. Faugeras, “An overview of the numerical methods for tokamak plasma equilibrium computation implemented in the NICE code”, Fusion Engineering and Design, 160 (2020), https://doi.org/10.1016/j.fusengdes.2020.112020
[9]: Blum, J. Numerical simulation and optimal control in plasma physics. 1989, John Wiley and Sons Inc, New York, NY (USA), ISBN 0-471-92187-4
[10]: Laurence, Peter and Edward Stredulinsky. "Convergence of a sequence of free boundary problems associated with the Grad variational problem in plasma physics." Communications on pure and applied mathematics 43.4 (1990): 547-573.
[11]: H. Heumann, A Galerkin method for the weak formulation of current diffusion and force balance in tokamak plasmas, Journal of Computational Physics, Volume 442 (2021), https://doi.org/10.1016/j.jcp.2021.110483.
[12]: G. Gros et al, Numerical simulation of tokamak plasma equilibrium evolution, Journal of Computational Physics, 529 (2025), https://doi.org/10.1016/j.jcp.2025.113849
[13]: Ambrosino, Giuseppe, et al. "XSC plasma control: Tool development for the session leader." Fusion engineering and design 74.1-4 (2005): 521-525. [7]: L.E. di Grazia et al., Fusion Engineering and Design, Vol. 192, p. 113631, 2023
[14]: Beghi, Alessandro, and Angelo Cenedese. "Advances in real-time plasma boundary reconstruction: from gaps to snakes." IEEE Control Systems Magazine 25.5 (2005): 44-64.
[15]: De Tommasi, Gianmaria. "Plasma magnetic control in tokamak devices." Journal of Fusion Energy 38.3 (2019): 406-436.
[16]: De Tommasi, G., et al. "Control of elongated plasmas in superconductive tokamaks in the absence of in-vessel coils."Nuclear Fusion 64.7 (2024): 076005.
[17] : di Grazia, Luigi Emanuel, et al. "Current limit avoidance algorithms for demo operation." Journal of Optimization Theory and Applications 198.3 (2023): 958-987.
[18]: De Tommasi, G., “Plasma Magnetic Control in Tokamak Devices”, Journal of Fusion Energy, 406-436, Vol 38, https://doi.org/10.1007/s10894-018-0162-5,
[19]: Zito, P., et al. "Design and realization of JT-60SA fast plasma position control coils power supplies." fusion engineering and design 98 (2015): 1191-1196
[20]: T. Wakatsuki et al 2024 Nucl. Fusion 64 10400
[21]: S. Inoue et al 2024 Nucl. Fusion 64 016014